Materials Evaluation

October 2008

Volume 66/Number 10

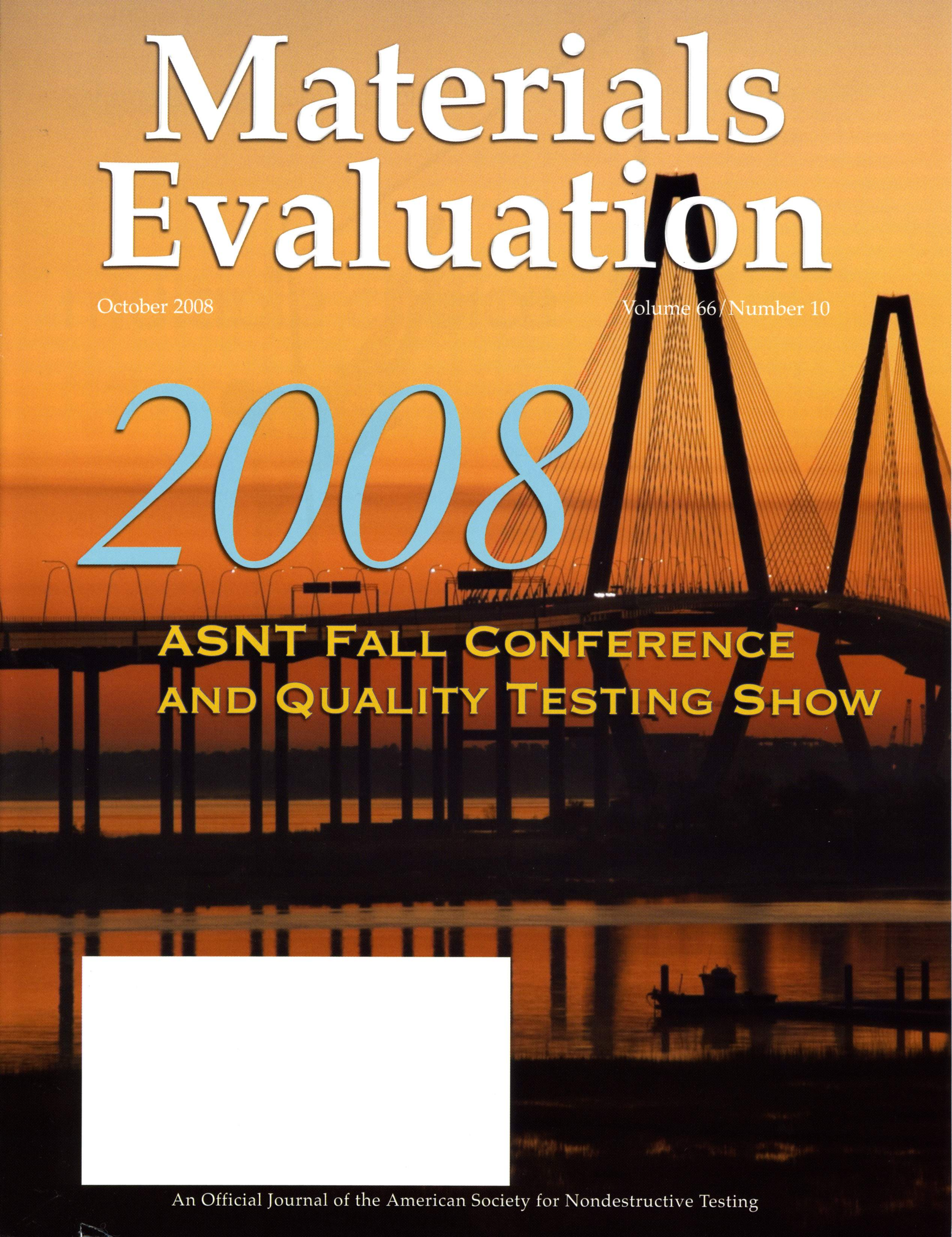

2008

ASNT Fall Conference and Quality Testing Show

An Official Journal of the American Society for Nondestructive Testing

Contents

Volume 66 / Number 10

Features

Technical Papers

Fall Conference

The 2008 ASNT Fall Conference and Quality Testing Show will be held 10-14 November in Charleston, South Carolina. Information on the conference can be found beginning on page 1000 of this issue of *Materials Evaluation.*

In This Issue

This issue includes information on the upcoming ASNT Fall Conference and Quality Testing Show, to be held November 10-14 in Charleston, South Carolina. The Exhibitors Gallery, featuring companies taking part in this year's show, begins on page 1013.

Inside ASNT

Departments

Ultrasound Vibrothermography Applications for Nondestructive Discontinuity Detection

by J.-M.A. Piau,* A. Bendada† and X.P.V. Maldague†

INTRODUCTION

In this paper, three application examples of nondestructive testing (NDT) utilizing ultrasonic vibrothermography are presented. The thermal signature of discontinuities is simpler to detect when the discontinuities themselves generate thermal emissions. Mechanical waves in the ultrasonic frequency range efficiently activate discontinuities to generate heat sources, which are then detected by an infrared camera.

VIBROTHERMOGRAPHY ULTRASONIC STIMULATION

Vibrothermography, also known as ultrasonic thermography (Dillenz et al., 2001) or thermosonics (Morbidini et al., 2007), utilizes mechanical waves to directly stimulate internal discontinuities instead of stimulating the surface, as with optical techniques. In vibrothermography, ultrasonic waves travel freely through a homogeneous material, wherein an internal discontinuity produces a complex combination of absorption, dispersion and scattering of the mechanical waves, whose principal manifestation will be in the form of heat. Heat, locally released, travels by conduction to the surface, and is then mapped spatially and temporally by a thermal infrared camera. The ultrasonic frequency range allows the stress level to be reduced with sufficient detectable thermal energy, contrary to the stress pattern analysis by thermal emission technique (Mountain and Webber, 1978), which uses a high stress level and low frequency. There are basically two stimulation techniques for vibrothermography similar to conventional optical techniques (Balageas et al., 1987; Maldague, 2001; Wu and Busse, 1998). The first technique consists of inducing ultrasound with a short time pulse at a constant amplitude. The second modulates the amplitude of the ultrasound. These two approaches are illustrated in Figure 1. It should be mentioned that with these two techniques, the ultrasonic stimulation can be modulated as well as the frequency (wobulation). Wobulation can prevent the activation of thermal standing wave patterns, which are encountered when the stimulation meets a natural frequency of the material. The ultrasonic wave is produced by a piezo transducer with a tip made of titanium that acts like a hammer. Hence, the part being tested should be firmly immobilized to avoid cantilever effects, clapping and sliding of the transducer. The transducer is pressed against the sample by two pneumatic pistons. For experimental repeatability, the pistons are digitally pressure controlled.

Even nanometric open cracks, invisible to other techniques, are revealed with vibrothermography.

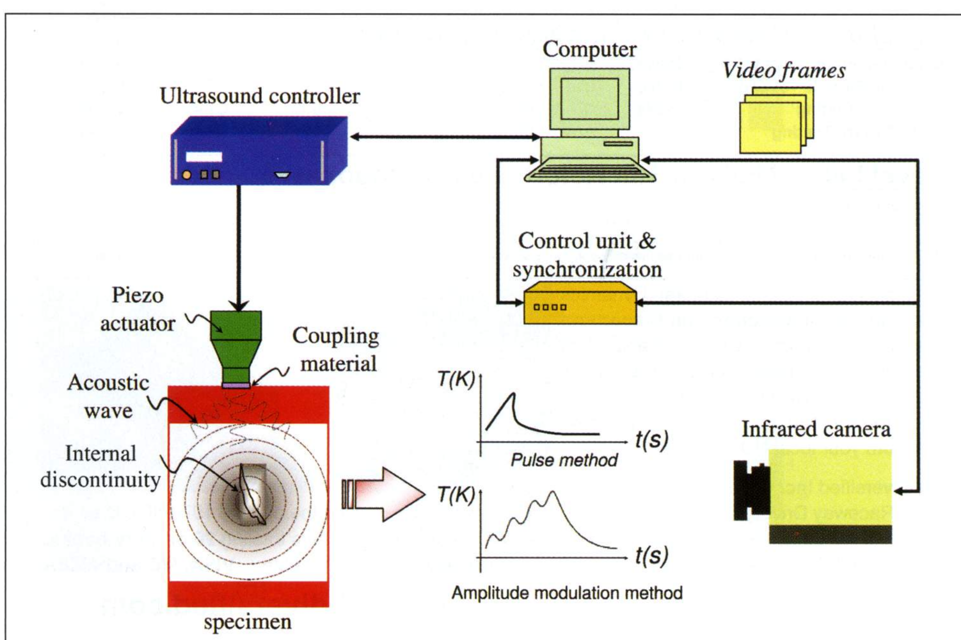

Figure 1 — Vibrothermography stimulated by ultrasound.

* Computer Vision and Systems Laboratory, Laval University, Quebec City, Quebec G1K 7P4, Canada; e-mail <jmpiau@axis-photon.com>.

† Computer Vision and Systems Laboratory, Laval University, Quebec City, Quebec G1K 7P4, Canada.

EXPERIMENTAL SETUP AND DATA ACQUISITION FOR VIBROTHERMOGRAPHY

The infrared camera used is operated in the spectral range of the middle infrared (3 to 5 µm). It has a spatial resolution of 512 × 640 and a high thermal resolution coded into 14 bits. The ultrasound source used for the experimentation is derived for an industrial plastic welder unit modified to generate elastic waves between 15 and 25 kHz. Figure 2 present the different parts of the ultrasound source. The horn is only attached to the booster if local energy is required. The in-house PC based software has been developed to generate various kinds of stimulation signals via a standard digital to analog PCI card. One analog signal controls the ultrasonic power amplitude, while the second signal is only used to generate the ultrasonic frequency sweep speed and range (wobulation). Synchronization of the stimulation and acquisition is achieved by a third signal from the same card. The stimulation duration varies from a few milliseconds in the pulse technique to several seconds in amplitude modulation. Thermal image acquisition starts slightly before the stimulation to record cold images, which are averaged and subtracted from the whole acquisition to improve detection contrast. Raw images occur often enough to highlight inhomogeneities in the specimen tested with the pulse technique. While the phase image is from a fast Fourier transform, image processing is required with the amplitude modulation technique.

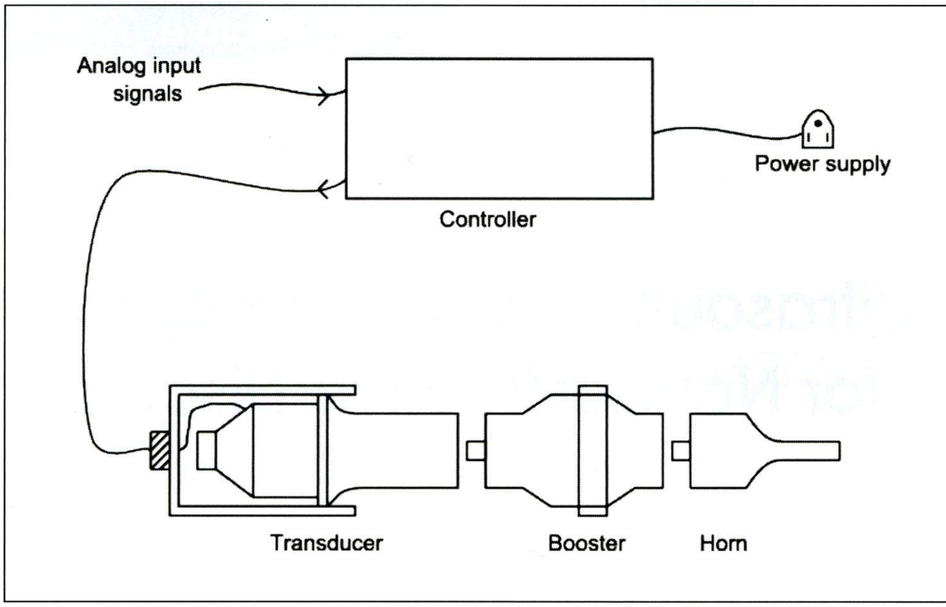

Figure 2 — Ultrasound system.

EXPERIMENTAL CONSIDERATIONS

A material between the booster and the sample is recommended not only as a coupling medium, but also to prevent damage to the sample surface. Poor coupling creates unwanted heat in the vicinity of the ultrasound induction point. Insulating the specimen from the testing bench improves the detection and reduces the power level to be induced. It is best to keep the ultrasonic wave within the specimen so that the wave does not spread everywhere. This can be done by placing cork slices wherever the specimen comes into contact with the test bench. The coupling pressure has a strong influence on the detection efficiency. A higher coupling pressure increases the detection efficiency; however, the risk of damaging the specimen then increases. The coupling pressure also maintains the specimen in place, which is important since the specimen should not move during stimulation. The thermal gradient observed at the specimen edges has to be considered with care; edges can be interpreted as material discontinuities. The final recommendation is to wear ear protection — despite the fact that ultrasound is beyond the human hearing capability, the nonlinear coupling (Han et al., 2002) creates audible frequencies.

DETECTION AND TESTING EXAMPLES

Vibrothermography is well suited to detect tiny cracks and delaminations in stratified composite materials. The first example presents the main landing gear of an F16, in which fatigue cracks were found. The second example is a fabricated test sample composed of a glass-reinforced fiber metal laminate containing inserts. Finally, a steel coated tungsten carbide coupon with crack formations resulting from a four point bending test is described.

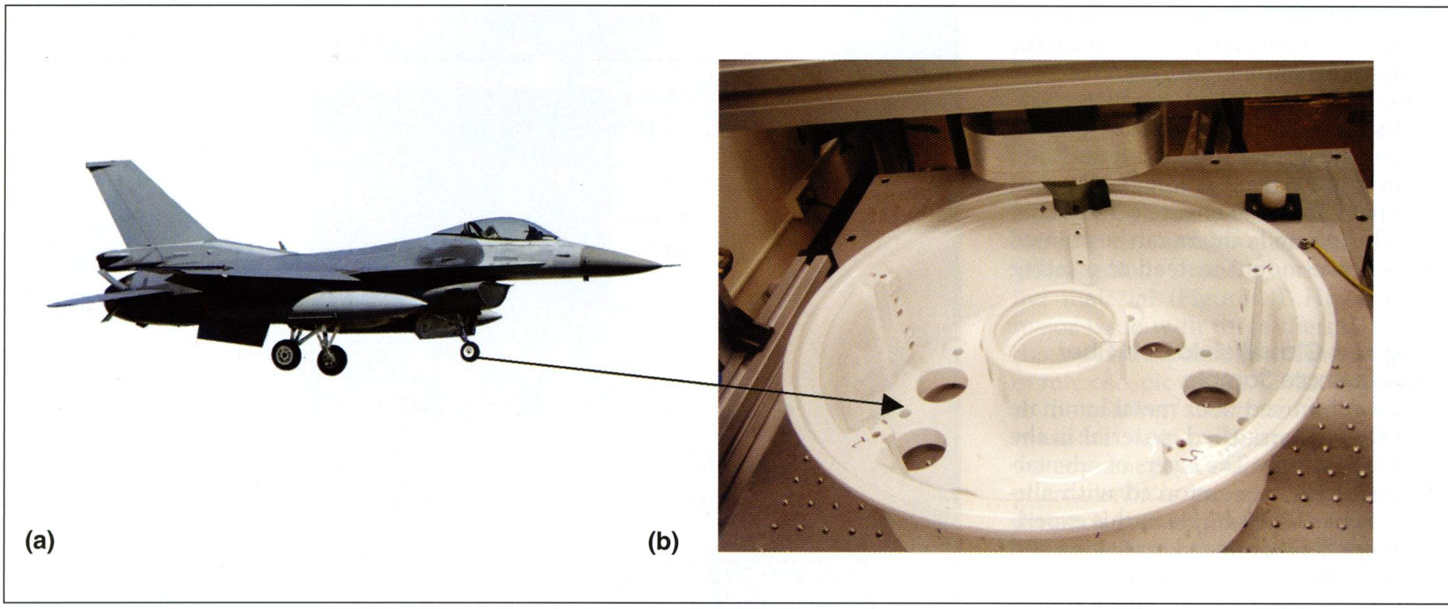

Figure 3 — The main landing gear of an F16: (a) on the aircraft; (b) in the experimental setup.

Testing of F16 Main Landing Gear

An F16 aircraft's main landing gear (Figure 3) was tested with low frequency ultrasound. Cracks are likely to appear at the brake mounts, which are equally spaced and numbered from one to five. The booster was pressed on the top edge of the rim (flat surface), as shown in Figure 3b. The wheel was tested without any conditioning, that is, no paint was applied to improve the emissivity. A 1378.95 kPa (200 psi) pressure was applied to couple the booster to the wheel, enough to keep the wheel in place while ultrasound was injected. The frequency range used ranged between 19.75 kHz and 21 MHz, the electrical power was set to 1.6 kW, and the maximum coupling efficiency did not exceed 10%. Amplitude modulation excitation with wobulation gave the best results.

The testing revealed that only the brake mount (number 5) did not have a fatigue crack. Cracks were detected at the bottom end of the brake mounts, and their location was circled on each of the phasegrams (Figure 4).

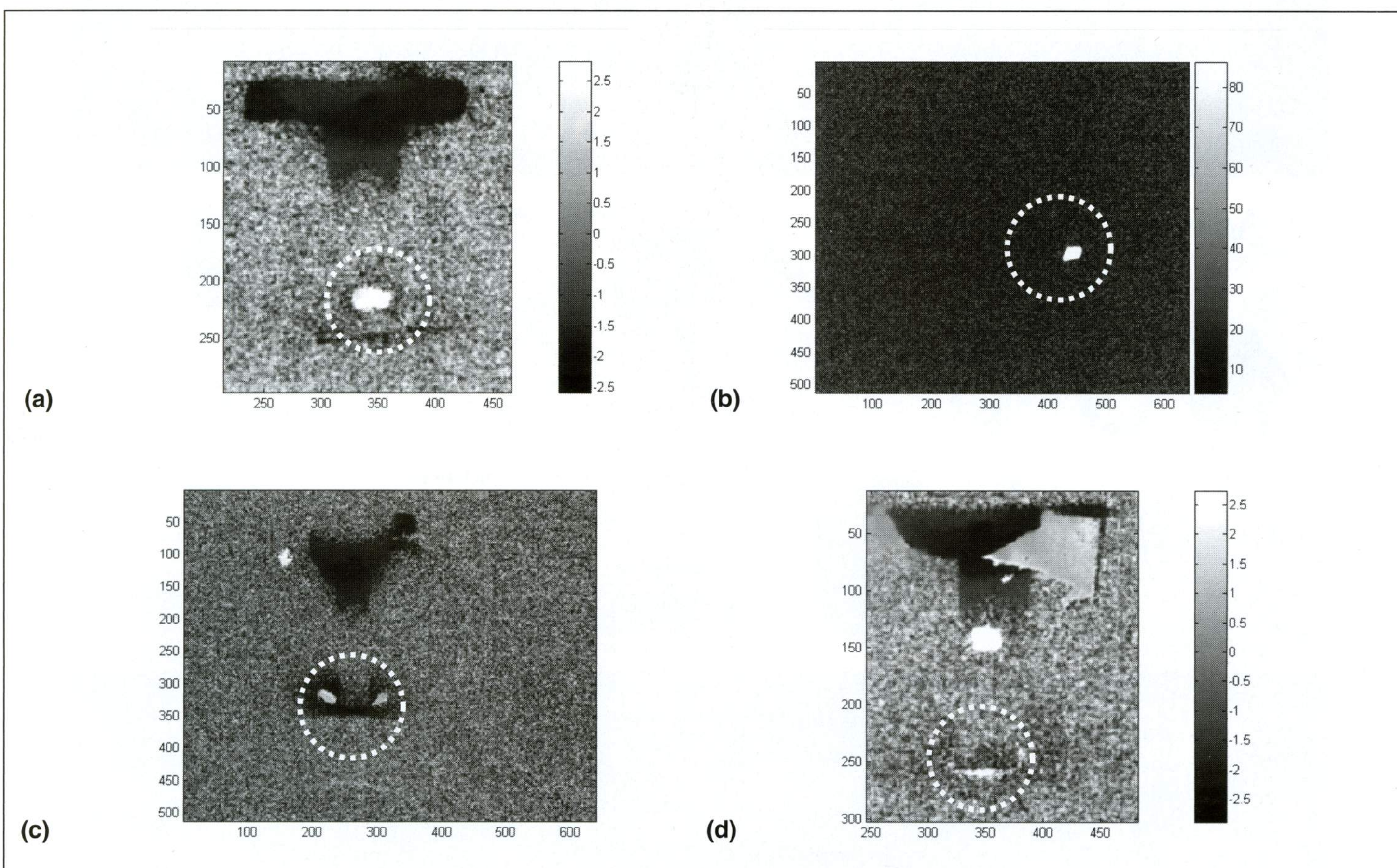

Figure 4 — Brake mount fast Fourier transform phasegram results: (a) brake mount 1; (b) brake mount 2; (c) brake mount 3; (d) brake mount 4.

Unwanted heat can be seen at the coupling surface where the booster lay on the rim edge. The landing gear, made of UNS A97050 (AMS 4340) alloy, conducts ultrasound very well, so the location chosen for the induction of the ultrasound into the rim is not critical as long as the surface is flat enough to ensure a good coupling. The infrared camera can be pointed at each brake mount instead of rotating the rim.

Testing of a Glass-Reinforced Fiber Metal Laminate Sample

Glass-reinforced fiber metal laminate is a fairly new stratified material in the aerospace industry. The layers of orientated glass fibers are reinforced with aluminum layers. The sample in this experiment is specially designed for testing and contains different materials inserted between layers (Figure 5). All inserts are located at the same depth. Inserts in columns 1 and 2 are released pieces of the layers, while a polyimide film and an aluminum material have been used as inserts in columns 3 and 4. Due to the cumbersome size of the booster compared to the sample size, ultrasonic waves have been induced on the side of the surface opposite the infrared camera (Figure 6). A wet

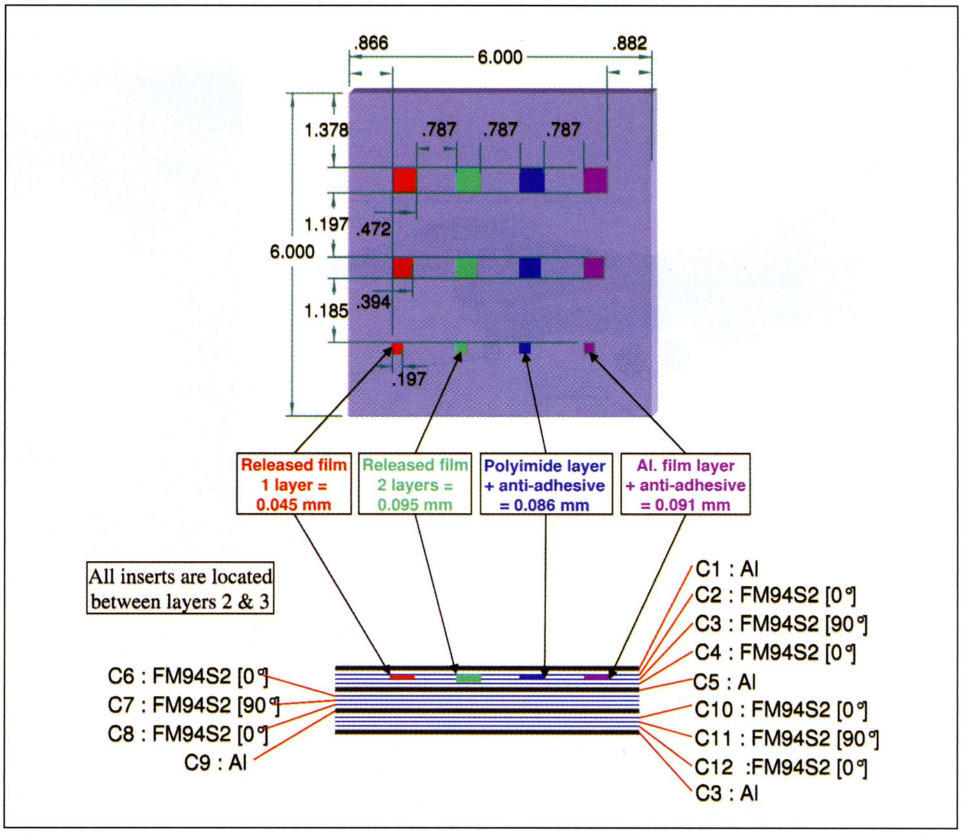

Figure 5 — Glass-reinforced fiber metal laminate sample specification.

conducts ultrasound very well; the induction locations chosen on the back side of the sample do not affect the detection.

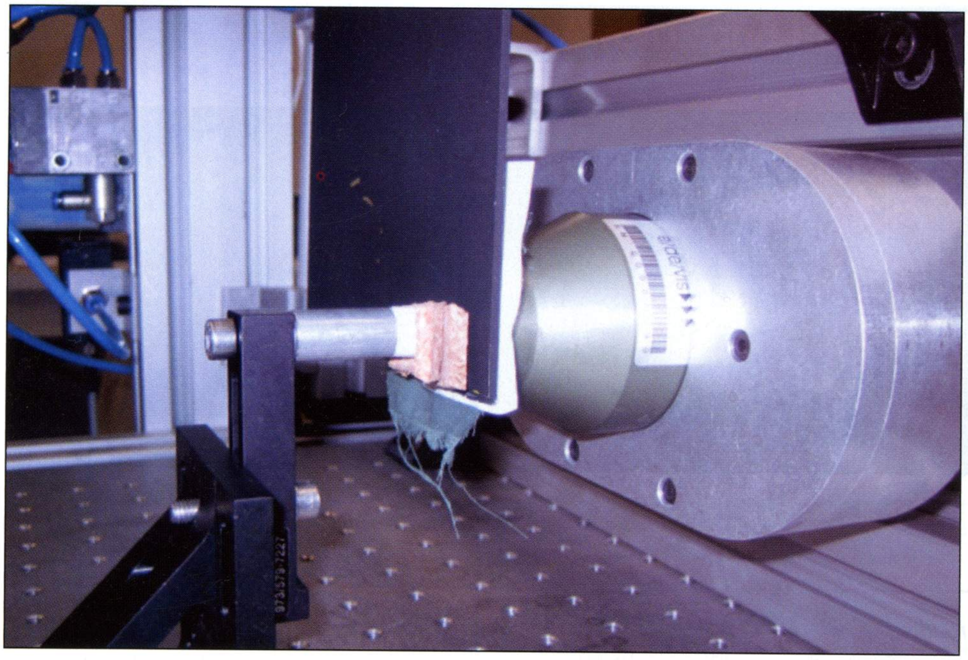

Figure 6 — Glass-reinforced fiber metal laminate specimen experimental setup.

Testing of Tungsten Carbide Coating

Recently, it has been shown that high velocity oxy fuel spraying of tungsten carbide or cobalt coatings onto steel substrates seems to be a suitable alternative to the environmentally unfriendly chromium coating material (Figure 8). However, one major issue with these thermal-sprayed coatings is the possibility of the appearance of microscopic cracks. Crack propagation to the coating/substrate interface might cause the coating to delaminate in between the adjacent open cracks. This disbonding phenomenon is strongly dependent on the distance between adjacent open cracks. Therefore, a nondestructive technique enabling the detection of cracks and the tracing of the evolution of their density is critical to preserve the components' integrity. Ultrasound is induced through the back of the specimen, as shown in Figure 9.

tissue couples the booster to the sample, with an additional layer of paper to protect against leaving tissue fiber traces on the black paint coating. The insulation consists of a hard aluminum post tipped with tetrafluoroethylene coating and a slice of cork. The insulation structure slightly masks a part of the testing view. Other experiments can be conducted by simply rotating the sample.

Single pulse stimulation at 20 kHz during 100 ms allows the temperature rise to be monitored for all inserts (Figure 7). The top row of inserts is the largest (472 × 472 µm [0.019 × 0.019 in.]) and the same observation was made on the second row (394 × 394 µm [0.016 × 0.016 in.]). On the bottom (197 × 197 µm [0.008 × 0.008 in.]), insert number 11 is barely revealed. A construction problem seems to have occurred for insert number 9, since two discontinuities appear instead of one, but this issue has been confirmed by conventional ultrasonic C-scan testing. The insulation point is clearly visible at the bottom and has no influence on detection. The insert geometry and dimensions correspond to the specification sheet, even though they are under a highly conductive aluminum layer. Glass-reinforced fiber metal laminate

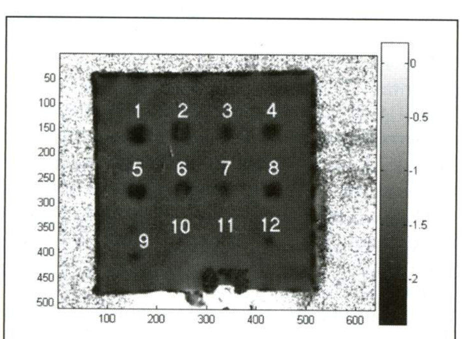

Figure 7 — Glass-reinforced fiber metal laminate phasegram.

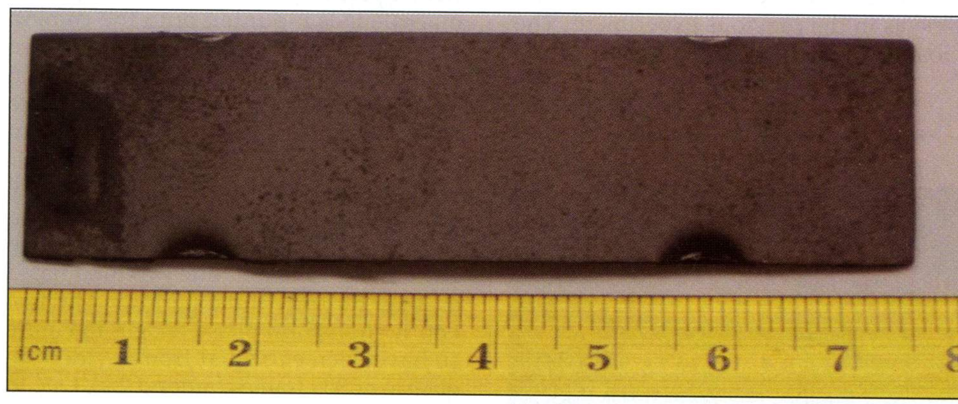

Figure 8 — Tungsten carbide coating sample.

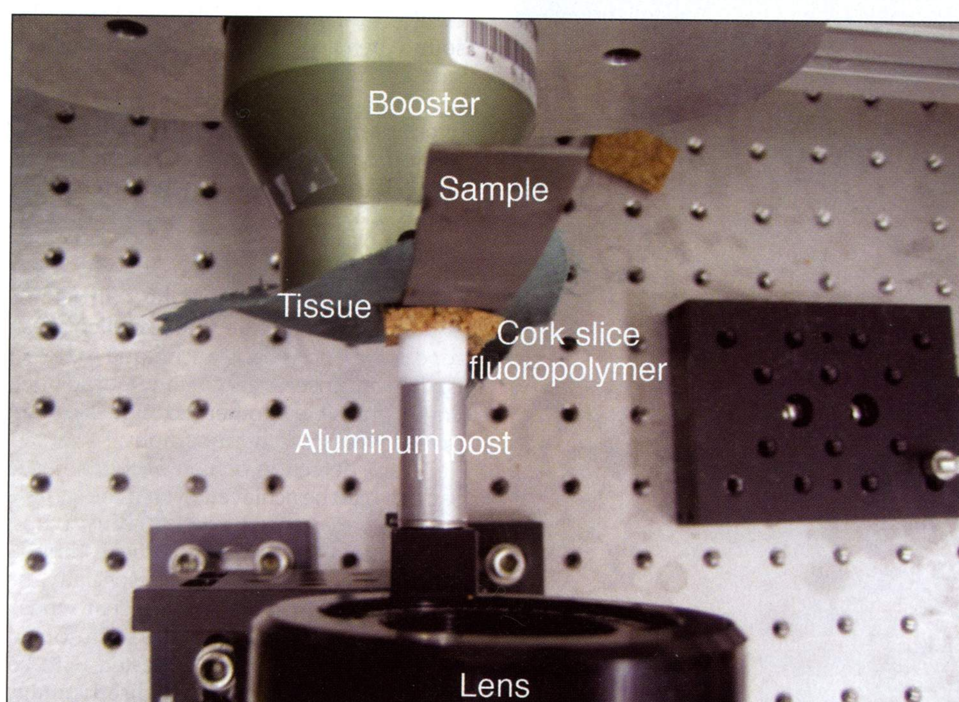

Figure 9 — Tungsten carbide coating specimen experimental setup.

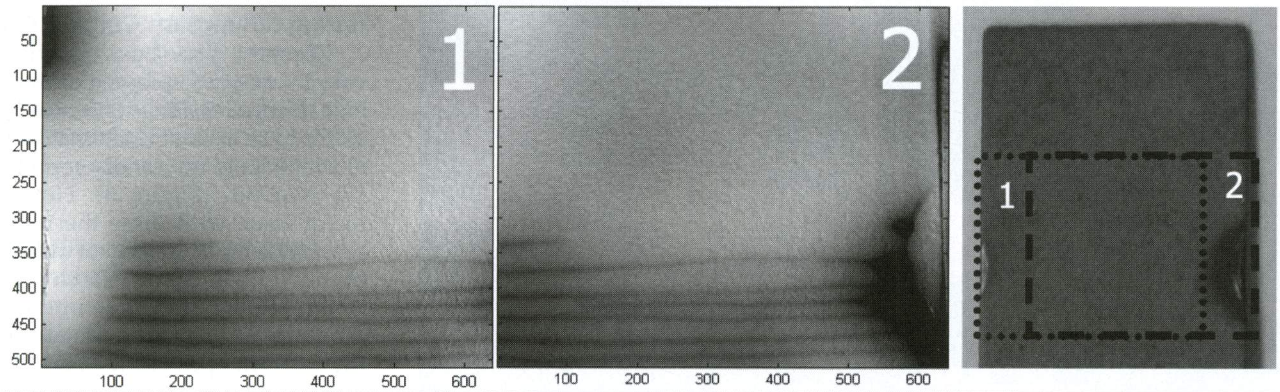

Figure 10 — Tungsten carbide coating phasegram results.

Coupling and insulation types are the same as in the previous experiment. The booster is pressed against the sample with a pressure of 344.74 kPa (50 psi). A macrolens is mounted onto the camera and only a small region of 16 × 12.8 mm (0.63 × 0.5 in.) is visualized; this spatial resolution of 25 µm is required because the crack spacing is on the order of 1 mm (0.04 in.). Amplitude modulation and pulse stimulation were suitable to reveal a thermal contrast.

The stimulation applied was set to 20 kHz and the amplitude was modulated at 2 Hz for only three periods. The fast Fourier transform phase images in Figure 10 have been extracted from a video sequence of 300 frames (around 2 s). Due to the limited field of view, two experiments were required to cover the sample width. Area 1 corresponds to the dotted box and Area 2 is the dashed box. One can see the cracks (horizontal dark lines) and the sound area above. The semicircles on each side are noncoated areas left by the holding points during the coating process. The overlapping area confirms well the reproducibility of the detection. Crack widths are on the order of a few nanometers (Piau et al., 2008).

CONCLUSION

The vibrothermography ultrasonic stimulation technique is an excellent, fast, repeatable and reliable technique to detect cracks and inserts. Even nanometric open cracks, invisible to other techniques, are revealed with vibrothermography.

Crack detection on complex geometric samples can be achieved even if the sample surfaces are coated with a shiny paint, while thermography with optical stimulation is very sensitive to heat, especially the brake mount inside a landing gear wheel. Novel materials such as glass-reinforced fiber metal laminate can be tested with vibrothermography. The only disadvantage of this NDT technique is that it functions by contact.

ACKNOWLEDGMENTS

This work was undertaken at Laval University and was supported by the Canada Research Chair: Multipolar Infrared Vision – Vision Infrarouge Multipolaire (MiViM). The authors thank Jean-Gabriel Legoux from the Industrial Materials Institute and Marc Genest from the Institute for Aerospace Research of the National Research Council of Canada for supplying the specimens used in the experimental work.

REFERENCES

Balageas, D.L., A.A. Déom and D.M. Boscher, “Characterization and Nondestructive Testing of Carbon-Epoxy Composites by a Pulsed Photothermal Method,” *Materials Evaluation*, Vol. 45, 1987, 461–465.

Dillenz, A., T. Zweschper and G. Busse, “Progress in Ultrasound Phase Thermography,” *Proceedings of SPIE*, Vol. 4360, 2001, pp. 574–579.

Han, X., W. Li, Z. Zeng, L.D. Favro and R.L. Thomas, “Acoustic Chaos and Sonic Infrared Imaging,” *Applied Physics Letters*, Vol. 81, 2002, pp. 3188–3190.

Maldague, X.P.V., *Theory and Practice of Infrared Technology for Nondestructive Testing*, Malden, Massachusetts, Wiley, 2001.

Morbidini, M., P. Cawley, T. Barden, D. Almond and P. Duffour, “Prediction of the Thermosonic Signal from Fatigue Cracks in Metals Using Vibration Damping Measurements,” *Insight*, Vol. 49, 2007, pp. 254–263.

Mountain, D.S. and J.M.B. Webber, “Stress Pattern Analysis by Thermal Emission (SPATE),” *Proceedings of SPIE*, Vol. 164, 1978, pp. 189–196.

Piau, J.-M., A. Bendada, X.P.V. Maldague and J.-B. Legoux, “Nondestructive Testing of Open Microscopic Cracks in Plasma-Sprayed-Coatings Using Ultrasound Excited Vibrothermography,” *Nondestructive Testing and Evaluation*, Vol. 23, 2008, pp. 109–120.

Wu, D. and G. Busse, “Lock-in Thermography for Nondestructive Evaluation of Materials,” *Revue generale de thermique*, Vol. 37, 1998, pp. 693–703.

Ω